



## Decadal cooling in the Indian summer monsoon after 1997/1998 El Niño and its impact on the East Asian summer monsoon

Kyung-Sook Yun,<sup>1</sup> Kyung-Ja Ha,<sup>1</sup> Bin Wang,<sup>2</sup> and Ruiqiang Ding<sup>3</sup>

Received 26 October 2009; revised 24 November 2009; accepted 14 December 2009; published 15 January 2010.

[1] Observational evidences are presented to show a significant atmospheric diabatic cooling in the Indian summer monsoon (ISM) region after the 1997/1998 El Niño. This study investigates the cause of this decadal cooling and its impact on the East Asian summer monsoon (EASM). After 1997/1998, the abnormal sea surface temperature warming in the western Pacific, which is not fully demonstrated in this study, induces enhanced local convection. This enhanced convection strengthens the Walker-type circulation and leads to moisture divergence, subsidence, and decreased cloudiness over the ISM, which in turn causes the diabatic cooling. The decadal cooling of the ISM, on the other hand, may affect the EASM through development of an anomalous local meridional cell over the EASM region and through enhancement of the Eurasian wave train pattern. Consequently, rainfall over the ISM and northern EASM decreases concurrently, while the southern EASM rainfall increases after 1997/1998.

**Citation:** Yun, K.-S., K.-J. Ha, B. Wang, and R. Ding (2010), Decadal cooling in the Indian summer monsoon after 1997/1998 El Niño and its impact on the East Asian summer monsoon, *Geophys. Res. Lett.*, 37, L01805, doi:10.1029/2009GL041539.

### 1. Introduction

[2] The Asian summer monsoon (ASM) plays an important role in modulating the water resources, agricultural affairs, and economic and societal activity. The ASM system consists of three sub-monsoon systems: East Asian summer monsoon (EASM), western North Pacific summer monsoon (WNPSM), and Indian summer monsoon (ISM) [Wang and LinHo, 2002]. Many monsoon studies have noted that the ASM system has experienced an abrupt decadal change and associated climate regime shift since 1993/94 extreme event over the East Asia [e.g., Ha *et al.*, 2009; Kajikawa *et al.*, 2009; Wang *et al.*, 2009; Qiu *et al.*, 2009]. The decadal change in the ASM rainfall is attributed to many contributing factors, such as the Tibetan Plateau warming, El Niño-Southern Oscillation (ENSO), and western North Pacific subtropical high [e.g., Chang *et al.*,

2000; Wang *et al.*, 2008]. In particular, the change of anomalous heating, as an important energy source for the atmospheric circulation, immediately affects the decadal change in monsoon variability. In addition, the anomalous heat source and sink may induce changes in remote regional monsoon rainfall via Rossby wave teleconnection pattern [e.g., Lu *et al.*, 2002].

[3] During 1997/1998 winter, the strongest El Niño event took place in the tropical Pacific and affected the Indian Ocean. The 1997/1998 ENSO showed rapid onset and termination [Takayabu *et al.*, 1999]. The unusual characteristics have motivated many researchers to investigate the dynamical heat changes (e.g., temperature advection, heat fluxes, and solar heating) responsible for the ENSO [e.g., Wang and McPhaden, 2001]. Recently, Harrison and Chiodi [2009] have marked the decadal change from pre- to post-1997/1998 in the character of sea surface temperature (SST) anomaly and its relationship with the westerly wind events in the tropical Ocean.

[4] In spite of the aforementioned evidence, the decadal change of monsoons after 1997/1998 remains unstudied partially due to the relatively short time period after 1998. Since diabatic heating in monsoon regions, particularly in the ASM region, is closely associated with ENSO, whether the decadal change before and after 1997/1998 has affected monsoon heating or not is one of our primary concerns. Furthermore, the impact of the change of the ISM heating on the EASM system is another target of our investigation. Both statistical analysis and simple model experiment will be used to fulfill our purpose.

### 2. Data and Model

[5] To investigate the decadal change in diabatic heating and circulation, we used the seasonal mean fields obtained from National Centers for Environmental Prediction/Department of Energy (NCEP/DOE) reanalysis for the period from 1979–2008 [Kanamitsu *et al.*, 2002], in which radiative transfer processes have been improved. The diabatic heating data are partitioned into six components: large scale condensation, deep convective, shallow convective, long-wave radiation, shortwave radiation, and vertical diffusion heating rates. The rainfall and SST data were obtained, respectively, from Climate Prediction Center Merged Analysis of Precipitation (CMAP) [Xie and Arkin, 1997] and BADC (British Atmospheric Data Centre) HadISST (Hadley Centre Sea Ice and Sea Surface Temperature data set) [Rayner *et al.*, 2003] for the period from 1979 to 2008.

[6] The model used in this study is a dry version of a linear Baroclinic model (LBM) with a horizontal resolution

<sup>1</sup>Division of Earth Environmental System, Pusan National University, Pusan, Korea.

<sup>2</sup>Department of Meteorology and International Pacific Research Center, School of Ocean and Earth Science and Technology, University of Hawai'i at Mānoa, Honolulu, Hawaii, USA.

<sup>3</sup>State Key Laboratory of Numerical Modeling for Atmospheric Sciences and Geophysical Fluid Dynamics, Institute of Atmospheric Physics, Chinese Academy of Sciences, Beijing, China.

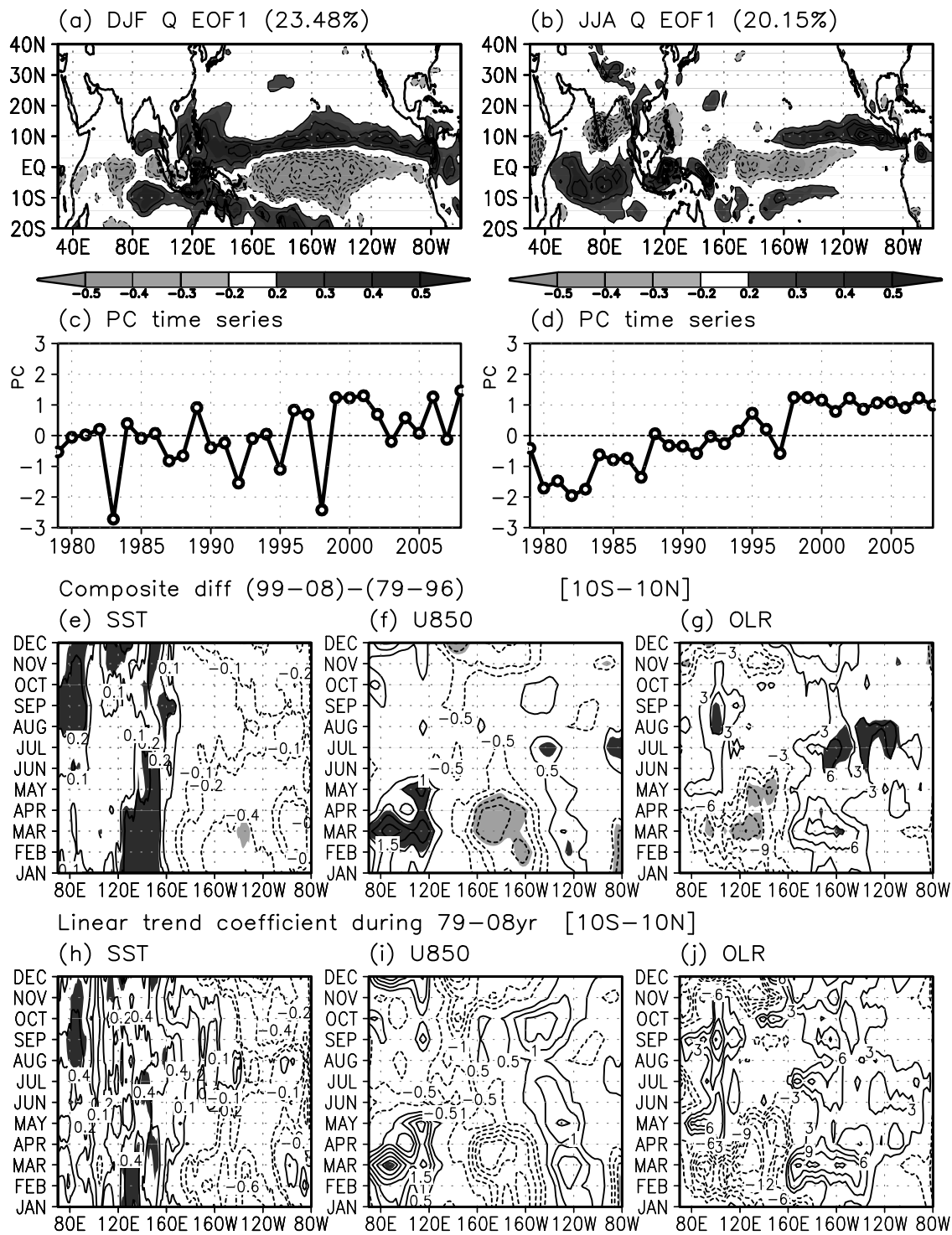


**Figure 1.** The (a and b) spatial patterns of the EOF1 and (c and d) its associated PC time series obtained from the vertically averaged diabatic heating data (K/day) during DJF (Figures 1a and 1c) and JJA (Figures 1b and 1d). The time-longitudinal section for (e–g) the composite difference between two periods for 1979–1996 and 1999–2008 and (h–j) linear trend coefficient (K/30-year) during 1979–2008 year of SST (Figures 1e and 1h), 850 hPa zonal wind (Figures 1f and 1i), and OLR anomalies (Figures 1g and 1j) averaged over the latitudinal range [10°S–10°N]. The shading in Figures 1e–1j indicates the anomaly significant at the 95% confidence level.

of T42 and 20 vertical levels, which is developed at the University of Tokyo’s Center for Climate System Research. In order to stress the role of dynamic processes, we purposely used a dry version of this model (i.e., the anomalous heat

source is prescribed as the forcing, excluding the moist source) in analyzing steady atmospheric response to a prescribed regional heat sink. The model was linearized about the climatological June–July–August mean basic state.

Reg of QV anomaly onto MAM OLR [120–150E, 5–20N]

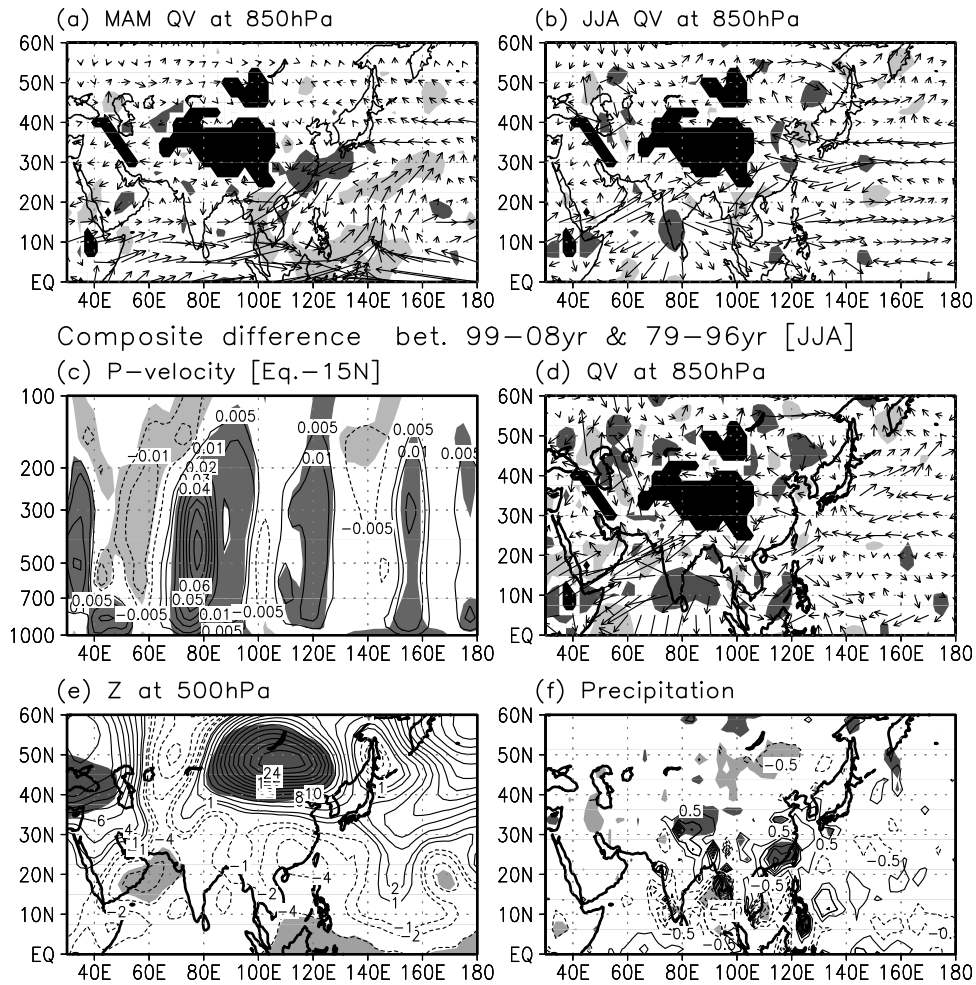


**Figure 2.** The regressed (a) MAM and (b) JJA moisture transport (arrow) and their divergence (shading) at 850 hPa against the MAM OLR anomalies averaged over [120°–150°E, 5°–20°N]. The composite difference of (c) vertical velocity (Pa/s) averaged over the latitude 0°–15°N, (d) 850 hPa moisture transport (arrow, m/s) and their divergence (shading,  $s^{-1}$ ), (e) 500 hPa geopotential height (m), and (f) precipitation (mm/day) anomaly between two periods for 1979–1996 and 1999–2008 during JJA. The shading indicates the anomaly significant at the 95% confidence level.

Details of the model are described by *Watanabe and Kimoto* [2000].

### 3. Decadal Cooling in the ISM After 1997/1998

[7] To detect the decadal change signals in the Asian-Pacific region, we have first performed Empirical orthogonal function (EOF) analysis of the vertically averaged diabatic heating in the domain [20°S–40°N, 30°E–60°W]. Figure 1 presents the first leading EOF mode obtained for boreal winter and summer, respectively. During winter, a strong cooling occurs in the equatorial eastern/central Pacific, while a remarkable warming appears in the western Pacific and regions surrounding the eastern Pacific cooling. In summer, the diabatic heating signal is similar to (but weaker than) that in winter, but over the southern ISM (SISM) and SCS summer monsoon (SCSSM) region, a significant diabatic cooling is observed. The ISM cooling is basically consistent with the decrease in the large-scale condensation and long-wave radiative heating components (not shown).

[8] It should be noted that the principal component (PC) time series in the diabatic heating experience a striking shift since 1997/1998 El Niño which has abrupt termination associated with the intensification of the easterly winds [e.g., *Takayabu et al.*, 1999]. The change in atmospheric heating is intimately linked to that in SST and the associated circulation. We have conducted the composite analysis of the time-longitude section of the SST, 850 hPa zonal wind, and OLR anomaly averaged over the equatorial zone (i.e., 10°S–10°N) between two periods (1999–2008 minus 1979–1996) (Figures 1e–1g). After the strong 97/98 El Niño, the regions of equatorial SST cooling (warming) correspond to well those of the decrease (increase) in the atmospheric diabatic heating. Significant easterly (westerly) anomalies are observed in the equatorial western/central Pacific (Indian Ocean) with a node around 120°E. It was reported that the anomalous easterly winds help a rapid termination of El Niño by generating upwelling Kelvin waves [e.g., *Kug and Kang*, 2006]. Consequently, the decadal easterly wind anomalies may prevent the full development

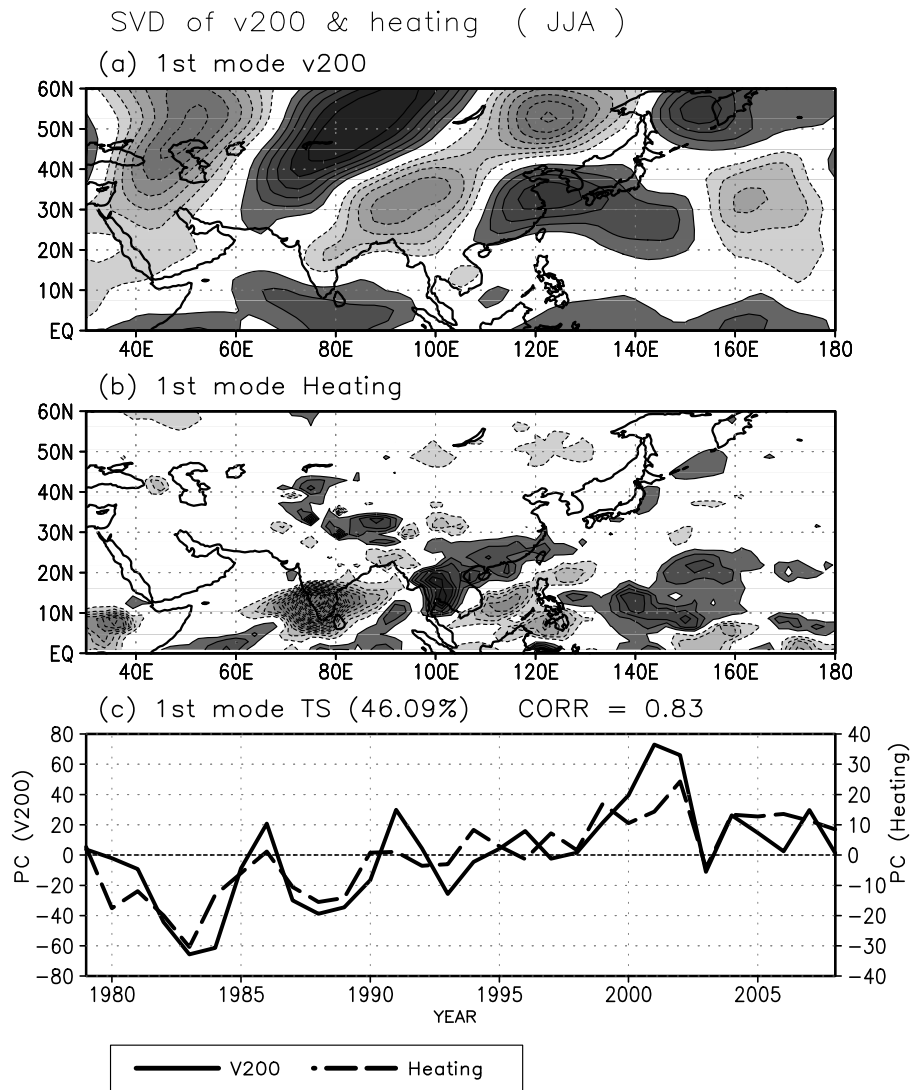


**Figure 3.** The Spatial pattern of the SVD1 between (a) the summer (JJA) mean meridional wind at 200 hPa (i.e., v200) and (b) the vertically averaged diabatic heating over the region  $[30^{\circ}\text{--}180^{\circ}\text{N}, 0^{\circ}\text{--}60^{\circ}\text{N}]$ . (c) The associated PC time series in the period 1979–2008.

of El Niño events since the strong 97/98 El Niño, and in turn, maintain remarkable cold anomalies in the eastern Pacific and warm anomalies in the western Pacific. The linear trend during the period of 1979–2008 year in the equatorial SST, zonal winds, and convection anomalies (Figures 1h–1j) does not exhibit a significant signal compared to the decadal change after 1997/1998 El Niño (Figures 1e–1g), although over the western Pacific they may share a local increase of SST. It reflects that the decadal change is more responsible for the warming in the western Pacific than the secure climate change.

[9] The abnormal SST warming in the western Pacific (Figure 1e) is responsible for the enhanced convective activity over the Philippine Sea and equatorial western Pacific (Figure 1g). The springtime enhanced convection over the Philippine Sea may play an important role in the recent atmospheric cooling in the ISM region. To examine this role, we have regressed the 850 hPa moisture transport ( $q\vec{V}$ ) and their divergence ( $\nabla \cdot q\vec{V}$ ) against the springtime OLR anomalies averaged over  $[120^{\circ}\text{E}\text{--}150^{\circ}\text{E}, 5^{\circ}\text{N}\text{--}20^{\circ}\text{N}]$

(Figures 2a and 2b). During the springtime, the enhanced convection induces strong moisture convergence in the western Pacific but moisture divergence in the Indian Ocean. During summertime, therefore, significant moisture divergence appears in the ISM region where the typical moisture convergence occurs during summer monsoon. In addition, the enhanced convection may contribute in part to the decreased cloudiness (i.e., suppressed convection and subsidence) over the ISM region, through modulating the atmospheric bridge (i.e., Walker circulation) [e.g., Alexander *et al.*, 2002].

#### 4. Change in the Circulation and Rainfall

[10] During summertime, a remarkable diabatic cooling appears over the ISM region, after the late 1990s (Figure 1b). To see the decadal change in circulation and precipitation before and after 1997/1998, we have made a composite analysis of the vertical pressure velocity (Pa/s), 850 hPa moisture transport (m/s), 500 hPa geopotential height (m),

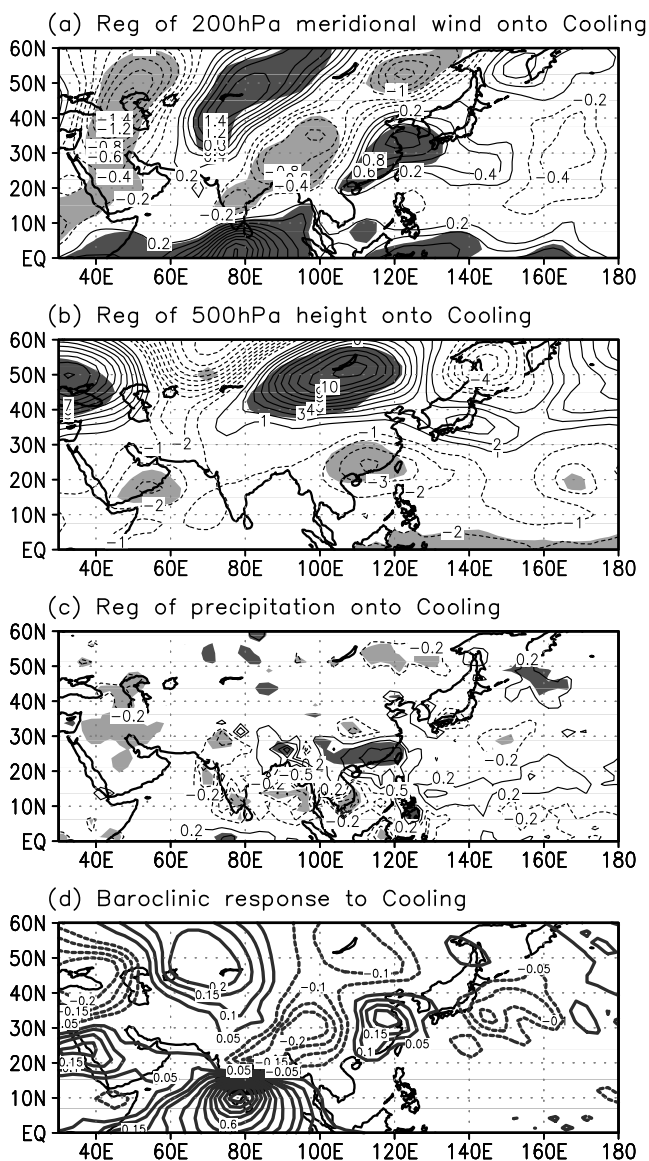


**Figure 4.** The regressed (a) 200 hPa meridional wind, (b) 500 hPa geopotential height, and (c) precipitation anomaly against the diabatic cooling averaged over  $[70^{\circ}\text{E}–90^{\circ}\text{E}, 10^{\circ}\text{N}–20^{\circ}\text{N}]$ . (d) The responses of the 200 hPa meridional wind anomaly (m/s) on day 15 to the initial forcing of the heat sink. The shading in Figures 4a–4c indicates the value significant at the 95% confidence level. The dark shading in Figure 4d denotes the initial forcing of the cooling.

and precipitation (mm/day) anomaly between two periods for 1979–1996 and 1999–2008 during the boreal summer (Figures 2c–2f). As noted above, after 1997/1998, a strong descending motion associated with anomalous Walker circulation occurs over the SISM ( $\sim 80^{\circ}\text{E}$ ) and SCSM ( $\sim 120^{\circ}\text{E}$ ) region (Figure 2c). The decadal change in the moisture transport is also revealed in the similar structure with the regressed field against the enhanced convection in the western Pacific (see Figures 2b and 2d). These results demonstrate that the decadal cooling in the ISM, which is primarily caused by the deficiency in the large-scale condensation and long-wave radiative heating, is related to the

decreases in the moisture convergence and cloudiness during the summer.

[11] It is conceivable that this diabatic cooling over the broad ISM region modulates the local meridional circulation. To the north of the diabatic cooling in the subtropics around  $\sim 25^{\circ}\text{N}$ , cyclonic circulation anomaly appears, and an anticyclonic anomaly occurred north of the cyclonic anomaly centered around  $50^{\circ}\text{N}$  (Figure 2e). Beneath the anomalous Mongolian high is suppressed precipitation (Figure 2f). Consequently, the deficient monsoon rainfall over the SISM and SCSM increases subtropical rainfall while reduces extratropical rainfall over the EASM region after 1997/1998 through change of the local meridional circulation.

[12] Another effect that could be induced by the ISM heat sink is seen in the Eurasian wave-like pattern (hereafter, EU pattern). The EU-like pattern along the subtropical jet stream is shown in 500 hPa geopotential height field (Figure 2e). Previous studies have reported that the ISM rainfall is related to the EU pattern [e.g., Lu *et al.*, 2002]. To confirm the linkage, we carried out a singular value decomposition (SVD) analysis in the domain  $[30^{\circ}\text{E}–180^{\circ}\text{E}, 0^{\circ}–60^{\circ}\text{N}]$  for the diabatic heating and 200 hPa meridional wind ( $v_{200}$ ) (Figure 3). Note that the  $v_{200}$  is more useful for describing the EU pattern, due to the fact that the  $v_{200}$  is little affected by the meridional shift of the jet stream [Lu *et al.*, 2002]. The first SVD mode explains about 46.1% of the total variance. The  $v_{200}$  pattern of the first SVD exhibits well-organized EU-like wavy structure along  $\sim 40^{\circ}\text{N}$ . The alternate pattern of southerly and northerly winds slightly tilts from southwest to northeast. The PC time series of the first SVD diabatic heating are significantly consistent with those of the first SVD  $v_{200}$ , which have a high correlation coefficient of  $\sim 0.83$ . In particular, both PCs exhibit abrupt changes from the negative phase into the positive phase after the late 1990s.

[13] The linkage of the ISM diabatic cooling on local meridional cell and EU pattern can be supported by the regression analysis of the  $v_{200}$ , 500 hPa geopotential height, and precipitation against the cooling anomaly averaged over the ISM region  $[70^{\circ}\text{E}–90^{\circ}\text{E}, 10^{\circ}\text{N}–20^{\circ}\text{N}]$  (Figures 4a–4c). The regressed fields bear a striking resemblance to the structure in decadal change before and after 1997/1998: the EU-like wave pattern is apparent in the regressed field of  $v_{200}$  anomaly (Figure 4a); in a reasonable consistence with the upper-level meridional wind, a strong anticyclonic (cyclonic) circulation appears in the northern (southern) part of China (Figure 4b); there exist reduced rainfall in the Indian monsoon, enhanced rainfall in the south China, and the decreased rainfall in the north China (Figure 4c).

[14] To confirm the impact of the ISM cooling on the EU pattern, we performed a simple numerical experiment with a dry version of LBM and the results are shown in Figure 4d. In the experiment, we imposed a cooling anomaly over the ISM region  $[70^{\circ}\text{E}–90^{\circ}\text{E}, 10^{\circ}\text{N}–20^{\circ}\text{N}]$ . The vertical structure of the initial heat forcing is basically in agreement with observed profile of the composite difference between the pre- and post-1997/1998 for diabatic heating centered at  $(80^{\circ}\text{E}, 15^{\circ}\text{N})$  (not shown). The horizontal structure of the  $v_{200}$  response induced by the ISM cooling on day 15 (the circulation response after day 15 has insignificant change with time) significantly resembles

that in the observed decadal change shown in Figures 3a and 4a. It reflects the development of the extratropical EU-like wave train caused by the ISM heat sink.

## 5. Conclusion and Discussion

[15] Since the strong 1997/1998 El Niño event, a significant change in diabatic heating is observed over the Asian-Pacific region. After 1997/1998, a significantly increased western Pacific SST warm anomaly from winter to spring leads to an enhanced convection in the western Pacific. The cause on this decadal change has not been firmly demonstrated in the present study. This enhanced convection induces moisture divergence and strong downward motion over SISM region and in turn the diabatic cooling anomaly over the ISM region. The heat sink in ISM affects significantly the EASM rainfall and circulation in two ways: One is the anomalous development of local meridional cell over the EASM; another is activation of EU-like wave pattern.

[16] The cooling in the ISM is primarily due to the deficient large-scale condensation and enhanced long-wave radiative cooling. The reduced long-wave heating in the middle atmosphere is coherent to the surface warming trend, which is associated with the increasing surface solar heating arising from decreased cloudiness (not shown). The problem on the radiative balance due to the recent increase in the anthropogenic greenhouse gases and atmospheric chemical component remains unsolved, which should be investigated in the future study. Although we could not explain fully why the decadal change in heating occurs after the 1997/1998 El Niño, this study provides the observed evidence of the decadal change after 1997/98 El Niño from the diabatic heating point of view. Understanding the impacts of abrupt climate changes in ASM, whatever their causes, would contribute to the improvement on the seasonal prediction in changed climate systems.

[17] **Acknowledgments.** We would like to thank M. Watanabe for providing the linear baroclinic model. This work was supported by the Ministry of Environment as “The Eco-technopia 21 project,” and the work was supported by the second stage of the Brain Korea 21 Project in 2009.

## References

- Alexander, M. A., I. Bladé, M. Newman, J. R. Lanzante, N. C. Lau, and J. D. Scott (2002), The atmospheric bridge: The influence of ENSO teleconnections on air-sea interaction over the global oceans, *J. Clim.*, 15, 2205–2231, doi:10.1175/1520-0442(2002)015<2205:TABTIO>2.0.CO;2.
- Chang, C.-P., Y. Zhang, and T. Li (2000), Interannual and interdecadal variations of the East Asian summer monsoon and tropical Pacific SSTs. Part I: Roles of the subtropical ridge, *J. Clim.*, 13, 4310–4325, doi:10.1175/1520-0442(2000)013<4310:IAIVOT>2.0.CO;2.
- Ha, K.-J., K.-S. Yun, J.-G. Jhun, and J. Li (2009), Circulation changes associated with the interdecadal shift of Korean August rainfall around late 1960s, *J. Geophys. Res.*, 114, D04115, doi:10.1029/2008JD011287.
- Harrison, D. E., and A. M. Chiodi (2009), Pre and post 1997/1998 westerly wind events and equatorial Pacific cold tongue warming, *J. Clim.*, 22, 568–581, doi:10.1175/2008JCLI2270.1.
- Kajikawa, Y., T. Yasunari, and B. Wang (2009), Decadal change in intra-seasonal variability over the South China Sea, *Geophys. Res. Lett.*, 36, L06810, doi:10.1029/2009GL037174.
- Kanamitsu, M., W. Ebisuzaki, J. Woollen, S. K. Yang, J. J. Hnilo, M. Fiorino, and G. L. Potter (2002), NCEP-DOE AMIP-II reanalysis (R-2), *Bull. Am. Meteorol. Soc.*, 83, 1631–1643, doi:10.1175/BAMS-83-11-1631(2002)083<1631:NAR>2.3.CO;2.
- Kug, J.-S., and I.-S. Kang (2006), Interactive feedback between ENSO and the Indian Ocean, *J. Clim.*, 19, 1784–1801, doi:10.1175/JCLI3660.1.
- Lu, R., J.-H. Oh, and B.-J. Kim (2002), A teleconnection pattern in upper-level meridional wind over the North African and Eurasian continent in summer, *Tellus*, 54A, 44–55.
- Qiu, Y., W. Cai, X. Guo, and A. Pan (2009), Dynamics of late spring rainfall reduction in recent decades over southeastern China, *J. Clim.*, 22, 2240–2247, doi:10.1175/2008JCLI2809.1.
- Rayner, N. A., D. E. Parker, E. B. Horton, C. K. Folland, L. V. Alexander, D. P. Rowell, E. C. Kent, and A. Kaplan (2003), Global analyses of sea surface temperature, sea ice, and night marine air temperature since the late nineteenth century, *J. Geophys. Res.*, 108(D14), 4407, doi:10.1029/2002JD002670.
- Takayabu, Y. N., T. Iguchi, M. Kachi, A. Shibata, and H. Kanzawa (1999), Abrupt termination of the 1997–98 El Niño in response to a Madden-Julian Oscillation, *Nature*, 402, 279–282, doi:10.1038/46254.
- Wang, B., and LinHo (2002), Rainy seasons of the Asian-Pacific monsoon, *J. Clim.*, 15, 386–398, doi:10.1175/1520-0442(2002)015<0386:RSOTAP>2.0.CO;2.
- Wang, B., Q. Bao, G. Wu, and Y. Liu (2008), Tibetan Plateau warming and precipitation changes in East Asia, *Geophys. Res. Lett.*, 35, L14702, doi:10.1029/2008GL034330.
- Wang, B., F. Huang, Z. Wu, J. Yang, X. Fu, and K. Kikuchi (2009), Multi-scale climate variability of the South China Sea monsoon: A review, *Dyn. Atmos. Oceans*, 47, 15–37, doi:10.1016/j.dynatmoce.2008.09.004.
- Wang, W., and M. J. McPhaden (2001), Surface layer temperature balance in the equatorial Pacific during the 1997–98 El Niño and 1998–99 La Niña, *J. Clim.*, 14, 3393–3407, doi:10.1175/1520-0442(2001)014<3393:SLTBIT>2.0.CO;2.
- Watanabe, M., and M. Kimoto (2000), Atmosphere-ocean thermal coupling in the North Atlantic: A positive feedback, *Q. J. R. Meteorol. Soc.*, 126, 3343–3369, doi:10.1002/qj.49712657017.
- Xie, P., and P. A. Arkin (1997), Global precipitation: A 17-year monthly analysis based on gauge observations, satellite estimates, and numerical outputs, *Bull. Am. Meteorol. Soc.*, 78, 2539–2558, doi:10.1175/1520-0477(1997)078<2539:GPAYMA>2.0.CO;2.

R. Ding, State Key Laboratory of Numerical Modeling for Atmospheric Sciences and Geophysical Fluid Dynamics, Institute of Atmospheric Physics, Chinese Academy of Sciences, Beijing 100029, China.

K.-J. Ha and K.-S. Yun, Division of Earth Environmental System, Pusan National University, Pusan 609-735, Korea. (kjha@pusan.ac.kr)

B. Wang, Department of Meteorology, School of Ocean and Earth Science and Technology, University of Hawai‘i at Mānoa, Honolulu, HI 96822, USA.